ARKIV FÖR FYSIK Band 15 nr 5

Read 12 November 1958

Contributions from thermal lattice defects to the energy content of Au, Ag, Cu and Al

By G. Borelius

With 10 figures in the text

1. Introduction and summary

In earlier papers surveyed recently (1) the present author tried to separate from the total energy content of a metal, the structural part due to thermal lattice defects on the assumption that the part due to lattice vibrations was approximately described by a Debye function. The structural energy thus obtained was used for a study of the relation between the solid and liquid states.

In the present paper we shall try a more elaborate determination of the energy due to thermal lattice defects in solid metals starting from the general assumption that the vibrational energy approaches the classical value $3RT$ with increasing temperature, avoiding the special assumptions contained in the Debye function. We shall also take into account the part of the energy content due to the free electrons, which was not done in the earlier calculations.

The results confirm the basic assumptions and allow a determination of the vibrational zero-point energy as well as the energy due to thermal lattice defects. The temperature dependence of the latter shows the existence of two different kinds of lattice defects. One of these which asserts itself first at high temperatures near the melting point is identified as lattice vacancies. Its energy of formation is of the order of magnitude calculated by Huntington and Seitz (2), Fumi (3), Seeger and Bross (4) and others, and determined by resistivity measurements on quenched metals by Bauerle, Klabunde and Koehler (5) and others. The other kind of defects represents the greater part of the structural energy. The same defects also seem to present themsleves in a calorimetric delay, following a rise of temperature, recently found by Åström (6). Their structure, which is still unindentified, will have to fulfil certain conditions found by the experiments.

2. Postulate for the vibrational energy

In order to separate from the total energy content of a metal the structural part due to thermal lattice defects we need theoretical expressions for the part of the energy due to the thermal vibrations of the atoms.

Our working hypothesis is that the sum of the vibrational zeropoint energy pro

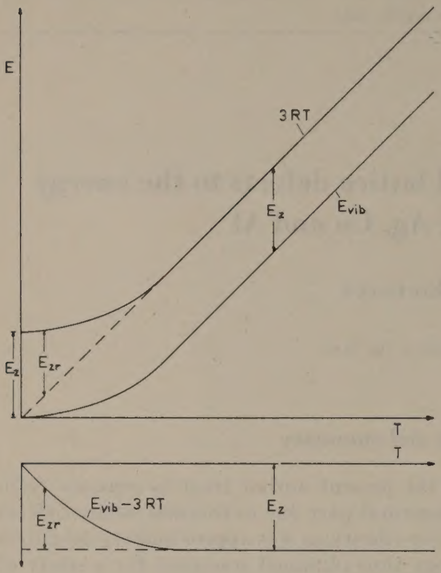

Fig. 1. Postulated scheme for the vibrational energy.

mole E_z and the thermal vibrational energy E_{vib} approaches the classical value $3RT$ with increasing temperature. Thus

$$E_z + E_{\text{vib}} \rightarrow 3RT \quad \text{for} \quad T \gg \theta, \tag{1}$$

where θ is a characteristic temperature of the metal. This condition is fulfilled by the Debye theory, in which E_{vib} is fully determined by T and a constant θ and the zero-point energy is $9R\theta/8$, but our assumptions are more general than those of the Debye theory, which are now known to be too narrow. Our hypothesis is at variance with those earlier theories which give a surplus energy due to the anharmonicity of the vibrations. Those theories, however, do not give any quantitative predictions for the deviations from the classical atomic heat capacity $3R$ and may perhaps be looked upon as an attempt to understand experimental results for which there was at that time no other explanation.

For our purposes we express the condition (1) in the form

$$E_z + E_{\text{vib}} = 3RT + E_{\text{zr}} \tag{2}$$

with the condition that the "residual zero-point energy" E_{zr} decreases from the value E_z for $T = 0$ to zero for $T \gg \theta$. These conditions are illustrated by the diagrams of fig. 1. Whether the residual zero-point energy E_{zr} can be theoretically separated as due to ordered vibrations or is just a formal difference is of no importance for our problems.

Our working hypothesis will be well supported by the results obtained in the following by its application to the measured energy content at normal practically zero pressure. A constant higher pressure or a pressure increasing with the temperature in order to keep the volume constant will surely alter the zero-point energy and the temperature dependence of the residual zero-point energy, but we have no reason to doubt that at high temperatures the total energy of vibrations approaches the value $3RT$ independent of pressure and volume.

3. Procedure of phenomenological analysis

For a determination of the structural energy due to thermal lattice defects, i.e. defects the concentrations of which are functions of the temperature, we have to start from the experimentally observed thermal energy per mole

$$E_{\text{obs}} = \int_0^T C\,dT, \tag{3}$$

where C is the atomic heat capacity at zero pressure or at a pressure of one atmosphere, which makes no observable difference. In a metal this observed energy is assumed to be the sum of three parts: the energy of the free electrons E_{el}, the thermal part E_{vib} of the energy of lattice vibrations, and the structural energy of thermal defects E_{str},

$$E_{\text{obs}} = E_{\text{el}} + E_{\text{vib}} + E_{\text{str}}. \tag{4}$$

The electron energy E_{el} is at low temperatures given by

$$E_{\text{el}} = \frac{\gamma}{2} T^2, \tag{5}$$

where the constant γ is known for many metals from experiment. Our only chance is to assume that this formula is approximately valid at all temperatures.

The total vibrational energy is the sum of the thermal part E_{vib} and the zero-point energy E_z. Our working hypothesis is that this sum approaches the classical value $3RT$ with increasing temperature.

From equations (2) to (5) we obtain the equation

$$E_{zr} - E_z + E_{\text{str}} = \int_0^T C\,dT - 3RT - \frac{\gamma}{2} T^2 \tag{6}$$

with known quantities on the right side and the unknown to the left. As will be seen in the following the variation of this sum with temperature is such that E_{str}, E_z and E_{zr} can be determined separately.

4. Gold

Gold is well adapted for a first demonstration of the use of an analysis by means of equation (6).

The first term to the right in this equation is obtained from calorimetric measurements. For the low-temperature range 0–300°K we have used the results of Geballe and Giauque (7). For the range from 300 to 600°K the increase of energy is taken

Table 1. Au. Energy data in cal/mole.

°K	E_{obs}	$3RT$	$\frac{\gamma}{2}T^2$	E_{zr}	E_{I}	E_{II}	$E_{\mathrm{obs-cal}}$
0	0	0	0	351			
15	0	89	0	262			
50	70	298	0	122			
100	293	596	1	46			
150	563	894	2	17			
200	849	1192	4	5			
250	1145	1490	5	0			+1
273	1283	1627	7		0		0
300	1445	1788	8		1		−1
400	2054	2384	14		8		−1
500	2675	2981	22		26		−3
600	3309	3577	31		55		−3
692	3914	4125	42		92	0	+6
905	5313	5395	71		200	3	−5
1073	6470	6396	100		296	22	+7
1232	7601	7344	132		389	88	−1
1273	7910	7588	141		413	128	−9

from a compilation by Stull and Sinke (8). For the range above 600°K we have used the measurements by Jaeger, Rosenbohm and Bottema (9) from which we have taken the directly determined energy differences between the high temperatures and room temperature. The total thermal energy values thus obtained for a number of temperatures are given as E_{obs} in table 1. It must be pointed out that the tables of energy values published by many authors, which are obtained by smoothing the observed values using power series of the temperature, are rather dangerous in our case because the smoothing often conceals the real dependence of temperature.

The third column of the table contains the values of $3RT$ and the fourth column the thermal energy of the free electrons, calculated with the value $\gamma = 1.74 \times 10^{-4}$ cal/mole deg^2 found by measurements on Au at low temperatures by Corak and Garfunkel (10).

The sums of the columns 2, 3 and 4, i.e. the values of the right hand side of equation (6), are plotted against the temperature in fig. 2. The curve is easily interpreted in terms of the left hand side of the equation. The initial decrease of the curve means the gradual disappearance of the residual zero-point energy E_{zr} in accordance with the scheme of the lower diagram in fig. 1. Because of the low Debye characteristic temperature $\theta = 190$ of Au, E_{zr} has practically disappeared before the rising of the curve due to the structural energy sets in. The horizontal part of the curve means that in this interval the atomic heat capacity has its classical value $3R$. The position of the horizontal line corresponds to the energy $-E_{\mathrm{z}}$. The zero-point energy comes out as $E_{\mathrm{z}} = 351$ cal/mole. Taking -351 as the zero point of a new scale, to the right of the diagram, the curves to the left and right give the residual zero-point energy E_{zr} introduced in column 5 of table 1, and the structural energy in cal/mole respectively.

The experimental points on the high temperature side still contain the original accidental errors from the measurements and are now graphically smoothed by a

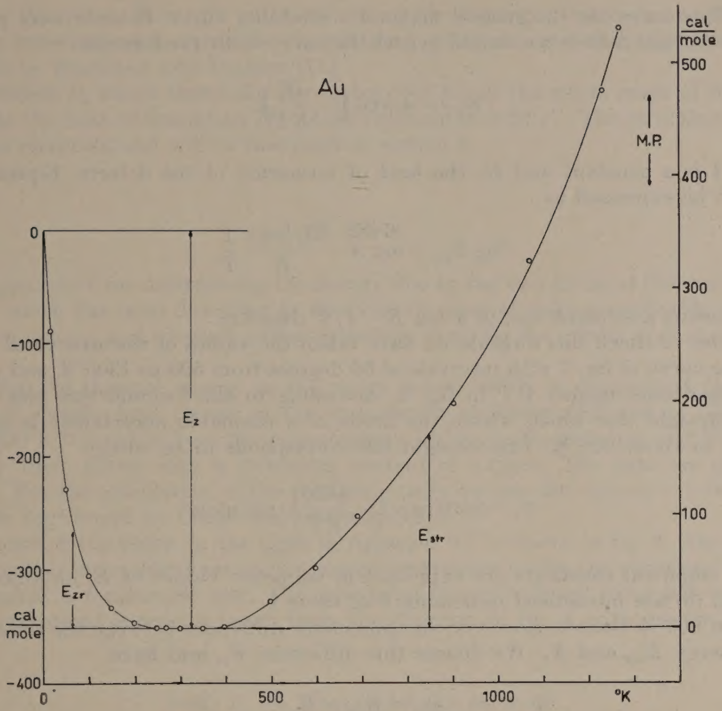

Fig. 2. Determination of structural energy af Au.

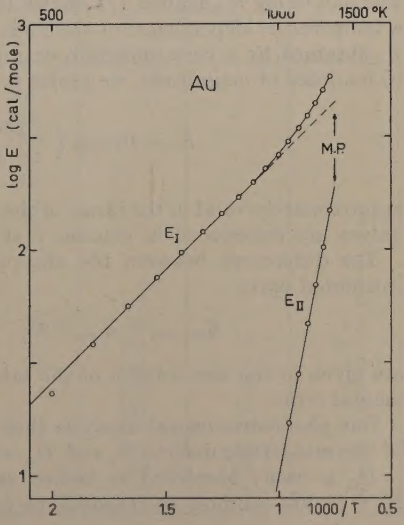

Fig. 3. Separation of the energy of the two kinds of defects in Au.

curve. This curve has the general shape of a solubility curve. If there were just one kind of thermal defects we should expect the curve to fit the formula

$$E_{\mathrm{str}} = A \exp\left(-\frac{H_f}{RT}\right), \tag{7}$$

where A is a constant and H_f the heat of formation of the defects. Equation (7) can also be expressed as

$$\log E_{\mathrm{str}} = \log A - \frac{H_f \log e}{R} \frac{1}{T} \tag{8}$$

which means a straight line in a $\log E - 1/T$ diagram.

In order to check this formula we have taken the values of the structural energy from the curve of fig. 2 with intervals of 50 degrees from 500 to 1300°K and plotted their logarithms against $1/T$ in fig. 3. According to the formula this plot should give a straight line which within the limits of a resonable uncertainty is also the case up to about 900°K. This straight line corresponds to an energy

$$E_{\mathrm{I}} = 2480 \exp\left(-\frac{4530}{RT}\right) \text{ cal/mole} \tag{9}$$

if both empirical constants are expressed in cal/mole. Values of E_{I} obtained from equation (9) are introduced in column 6 of table 1.

Above 900°K there is, however, an appreciable difference between the total structural energy E_{str} and E_{I}. We denote this difference E_{II} and have

$$E_{\mathrm{II}} = E_{\mathrm{str}} - E_{\mathrm{I}}. \tag{10}$$

The plot of $\log E_{\mathrm{II}}$ against $1/T$ shown in fig. 3 gives again a straight line which means a temperature dependence of the form of equation (7). As in this case the constant A, obtained by a very uncertain extrapolation to $1/T = 0$, would be uncertain even to its order of magnitude, we prefer to give the result in the formula

$$E_{\mathrm{II}} = 10 \exp\left(-\frac{23000}{R}\left(\frac{1}{T} - \frac{1}{1000}\right)\right) \text{ cal/mole} \tag{11}$$

approximately valid in the range of the measurements. From this equation calculated values are introduced in column 7 of table 1.

The differences between the observed thermal energy E_{obs} and the sum of its calculated parts

$$E_{\mathrm{obs-cal}} = E_{\mathrm{obs}} + E_{\mathrm{z}} - E_{\mathrm{zr}} - E_{\mathrm{el}} - 3RT - E_{\mathrm{I}} - E_{\mathrm{II}} \tag{12}$$

are given in the last column of the table. They are well within the limits of experimental error.

Our phenomenological analysis thus shows the existence of two different species of thermal lattice defects D_{I} and D_{II} with the thermal energies E_{I} and E_{II}.

D_{II} is easily identified as lattice vacancies. The empirical energy of formation $H_f = 23\,000$ cal/mole corresponds to 1.0 eV which within the limits of error is the same as the value $H_f = 1.02 \pm 0.06$ eV found by Bauerle, Klabunde and Koehler (5) from resistivity measurements on quenched specimens, and the value 0.95 ± 0.1 reported by Bradshaw and Pearson (11).

The defect D_{I} which thermally dominates over D_{II} in the whole range of the solid state has the heat of formation $H_f = 4530$ cal/mole or 0.20 eV. The structure of this defect is unknown and will be discussed in section 8.

5. Silver

The procedure for determining the energy due to the two kinds of thermal lattice defects which has been described in detail in the case of gold is applicable also for the other metals, and we shall confine ourselves to giving the results in diagrams and tables.

For Ag the thermal energy in the range below 300°K is determined from the values of specific heat chosen in the compilation of Kelley (12) and in the range above 300°K it is taken from the measurements of Jaeger, Rosenbohm, and Weenstra (13) on their silver with a minimum content of oxygen. The data are given in table 2. For the calculation of the electron energy we use the value $\gamma = 1.48 \times 10^{-4}$ cal/mole deg² found by Corak and Garfunkel (10).

The sum of the terms to the right in equation (6) is shown in fig. 4. Also in Ag, with $\theta = 215$, the residual zero-point energy disappears before the structural energy has reached a measurable size. The zero-point energy is found to be 403 cal/mole.

The structural energy is taken from the diagram of fig. 4 with intervals of 50

Table 2. Ag. Energy data in cal/mole.

°K	E_{obs}	$3RT$	$\frac{\gamma}{2}T^2$	E_{zr}	E_{I}	E_{II}	$E_{\mathrm{obs-cal}}$
0	0	0	0	403			
20	4	119	0	288			
50	52	298	0	157			
100	252	596	1	58			
150	512	894	2	19			
200	795	1192	3	3			
250	1091	1490	5	0			−4
273	1230	1627	6				0
300	1395	1788	7		0		+3
374	1839	2229	10		4		−1
573	3084	3416	24		47		0
671	3725	4000	33		90		+5
790	4512	4709	46		161	0	−1
902	5282	5377	60		244	2	+2
975	5791	5812	70		303	6	+3
1022	6128	6092	77		342	12	+8
1074	6494	6402	85		387	23	0
1123	6846	6694	93		431	41	−10
1168	7196	6963	101		468	63	+4
1213	7547	7231	109		512	101	−3

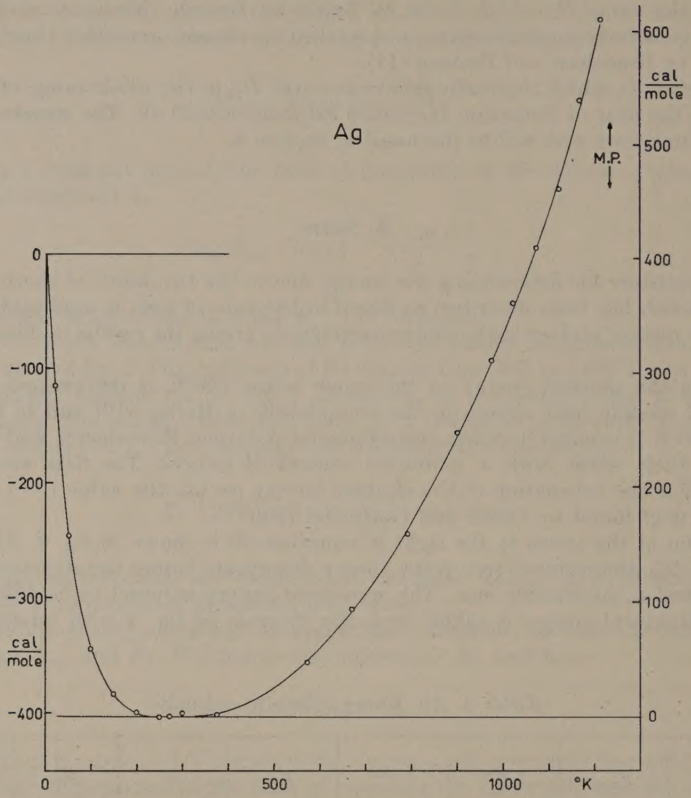

Fig. 4. Determination of structural energy of Ag.

degrees from 500 to 1200°K and the logarithms are plotted against $1/T$ in fig. 5. The analyzis of this plot has given for the first kind of defect the energy

$$E_{\mathrm{I}} = 4370 \exp\left(-\frac{5160}{RT}\right) \text{ cal/mole.} \tag{13}$$

The energy due to the second kind of defect, identified with the vacancies, is about 8.9 cal/mole at $T = 1000$ and the slope of the line drawn in fig. 5 gives the heat of formation $H_f = 27\,500$ cal/mole. We have thus

$$E_{\mathrm{II}} = 8.9 \exp\left(-\frac{27500}{R}\left(\frac{1}{T} - \frac{1}{1000}\right)\right) \text{ cal/mole.} \tag{14}$$

$H_f = 27\,500$ cal/mole corresponds to 1.2 eV.

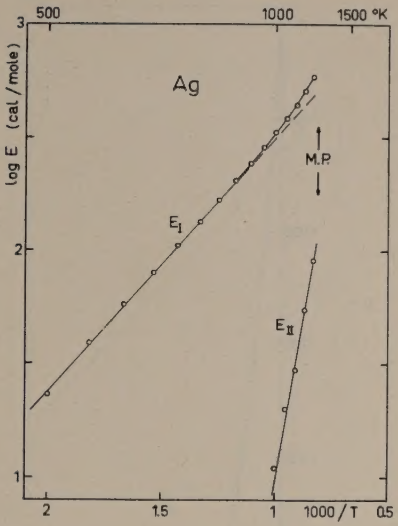

Fig. 5. Separation of the energy of the two kinds of defects in Ag.

6. Copper

Up to 300°K the experimental energy values in table 3 are based on measurements by Giauque and Meads (14) and from 300° to 500°on Stull and Sinke's compilation of heat-capacity data (8). Above 500° we have used the results of Jaeger, Rosenbohm and Bottema (15). Unfortunately these authors have not published their results near to the melting point which is at 1083°C. In a foot note they say that

Table 3. Cu. Energy data in cal/mole.

°K	E_{obs}	$3RT$	$\frac{\gamma}{2}T^2$	E_{zr}	E_{I}	E_{II}	$E_{\text{obs-cal}}$
0	0	0	0	602			
15	0	119	0	483			
50	21	298	0	325			
100	161	596	1	166			
150	383	894	2	89			
200	645	1192	3	52			
250	923	1490	5	30			
273	1056	1627	6	25	0		
300	1213	1788	7	19	1		
400	1807	2384	13	6	6		
500	2415	2981	20	2	24		
586	2963	3495	28	0	42		0
693	3650	4130	38		80	0	+4
904	5033	5388	65		183	4	−5
1072	6186	6389	92		279	22	+6
1233	7309	7347	122		377	71	−6

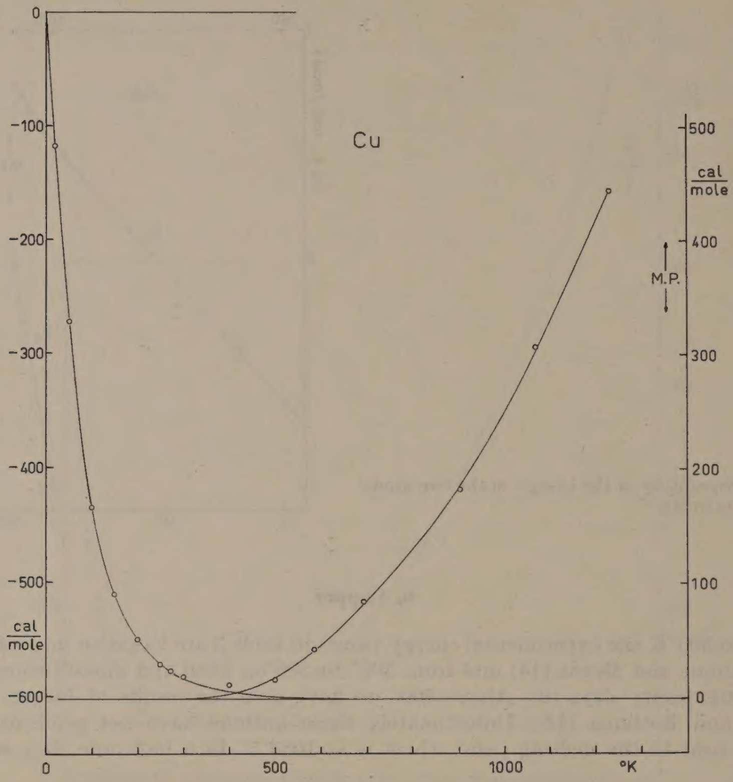

Fig. 6. Determination of the structural energy of Cu.

"above 960° copper evidently shows an abnormal behaviour: its specific heat then increases more rapidly with the temperature. The result will be discussed in a later paper". We have found no such paper. The results would probably have been of good use for a better determination of the vacancy energy, which in fact can be expected to raise the specific heat rapidly in this range of temperature. For γ we have used the value 1.60×10^{-4} cal/mole deg^2 found by Corak and Garfunkel (10).

As copper has a high Debye characteristic temperature of about $\theta = 325$, the falling curve of the residual zero-point energy and the rising curve of the structural energy in fig. 6 overlap slightly, which gives an extra uncertainty to the estimated zero-point energy, $E_z = 602$ cal/mole, of a few units.

The energy functions for the two kinds of defects obtained from the lines in fig. 7 are

$$E_{\mathrm{I}} = 2750 \exp\left(-\frac{4950}{RT}\right) \text{ cal/mole} \tag{15}$$

and

$$E_{\mathrm{II}} = 12 \exp\left(-\frac{19000}{R}\left(\frac{1}{T} - \frac{1}{1000}\right)\right) \text{ cal/mole.} \tag{16}$$

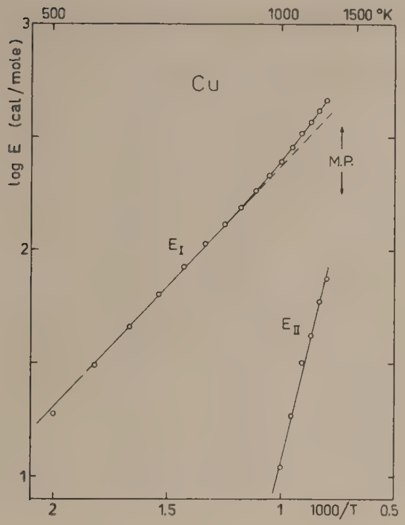

Fig. 7. Separation of the energy of the two kinds of defects in Cu.

The energies of formation correspond to $H_f = 0.22$ eV for the main defects and $H_f = 0.8$ eV for the vacancies. The latter value agrees fairly well with theoretical predictions of $H_f = 1$ eV by Huntington and Seitz (2), 0.9 eV by Fumi (3) and 0.8 eV by Seeger and Bross (4).

7. Aluminium

For Al we have found no directly useable calorimetric determinations of the energy content at high temperatures. We are restricted to the compiled and smoothed values given by Kelley (12) and Stull and Sinke (8) shown in table 4. The results give therefore only a rough orientation. For γ we have used the value $\gamma = 3.484 \times 10^{-4}$ cal/mole deg² found by Kok and Keesom (16).

Al has a very high Debye temperature of about $\theta = 400$ which leads to an appreciable overlapping of the falling and rising curves in fig. 8. Our estimation of the zero-point energy gives 730 cal/ mole. The analysis of the structural energy illustrated by fig. 9 gives the empiric formulae

$$E_{\mathrm{I}} = 4040 \exp\left(-\frac{4720}{RT}\right) \text{ cal/mole} \tag{17}$$

and

$$E_{\mathrm{II}} = 7 \exp\left(-\frac{13000}{R}\left(\frac{1}{T} - \frac{1}{750}\right)\right) \text{ cal/mole.} \tag{18}$$

The heats of formation 4720 and 13 000 cal/mole correspond to 0.20 and 0.56 eV. The value $H_f = 0.56$ eV for the formation of vacancies is in fair agreement with values obtained from recent resistivity measurements on quenched specimens. From

Table 4. Al. Energy data in cal/mole.

T	E_{obs}	$3\,R\,T$	$\frac{\gamma}{2}\,T^2$	E_{zr}	E_{I}	E_{II}	$E_{\text{obs}\,\cdot\,\text{cal}}$
0	0	0	0	730			
20	0	119	0	611			
50	12	298	0	444			
100	117	596	2	249			
150	310	894	4	142			
200	551	1192	7	82			
250	820	1490	11	49	0		
273	950	1627	13	40	1		
300	1105	1788	16	30	1		
400	1703	2384	28	10	11		
500	2330	2981	44	0	35	0	0
600	2987	3577	63		77	2	+2
700	3674	4173	85		136	10	0
800	4391	4769	112		208	32	0
900	5137	5365	141		289	77	−5

the extrapolated initial increments of resistivity after quenching from different temperatures obtained from diagrams published by Panseri, Gatto and Federighi (17) we obtain $H_f = 0.5$ eV. De Sorbo and Turnbull (18) report a value in excess of 0.6 eV. Bradshaw and Pearson (19) report the value 0.76 eV.

8. The determination by Åström of heat of formation of lattice defects

We have found that the temperature variations of the heat content of metals reveal the existence of two different thermal defects denoted D_{I} and D_{II}. D_{II} has been identified with the defects which are preserved for some time after quenching from high temperatures and which are theoretically interpreted as vacancies. D_{I} is the thermally dominating defect in the whole range of the solid state. As pointed out earlier by the present author the phenomenon of melting is also dominated by an increase of some defects other than vacancies, which evidently are the D_{I}-defects. Contrary to the D_{II}, the D_{I} are not, at least not to any great extent, preserved by quenching. On the other hand recent measurements in this laboratory by Åström (6) have given the surprising result that in very pure and coarse-grained metals after an increase of the temperature the development of certain defects is slow enough to be studied by isothermal calorimetry. A discussion of different possibilities gave as the most probable interpretation that these defects were a part of the unindentified defects causing the increase of structural energy discussed in earlier papers of the present author. We are now able to give further evidence that the defects studied by Åström are the D_{I}-defects.

In the log $E - 1/T$ diagrams for Ag of fig. 10 the line marked E_{I} is the same as in fig. 5 and the other lines are those obtained by Åström. Åström had found that when specimens of pure Ag were heated from room temperature to various temperatures in the range 100 to 400°C, the heat taken up in order to obtain equilibrium at the new

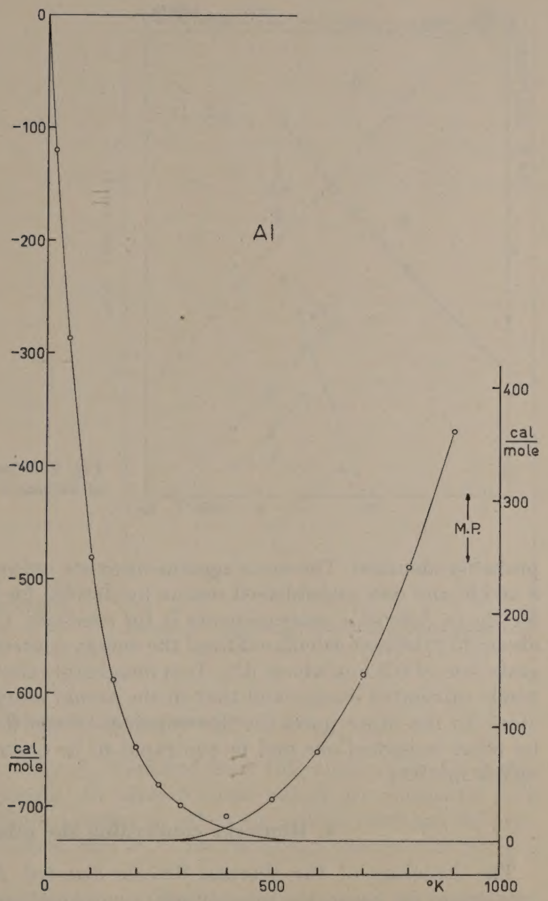

Fig. 8. Determination of the structural energy of Al.

temperature has an exponential tail with a time constant of a few hours. The energy E_t contained in these tails increases with increasing temperature as

$$E_t = A_t \exp\left(-\frac{H_f}{RT}\right) \tag{19}$$

where H_f is a heat of formation and A_t a constant increasing with increasing purity and grain size of the specimen. In a diagram of the type of fig. 10 this gives straight lines. The figure shows such lines for three specimens of 99.999 % Ag with the grain size increasing from A to C. At least for the specimen C the slope of the line is the same within the limits of error as that of the line now obtained from the energy content. This means that the energy of formation is the same and the defects most

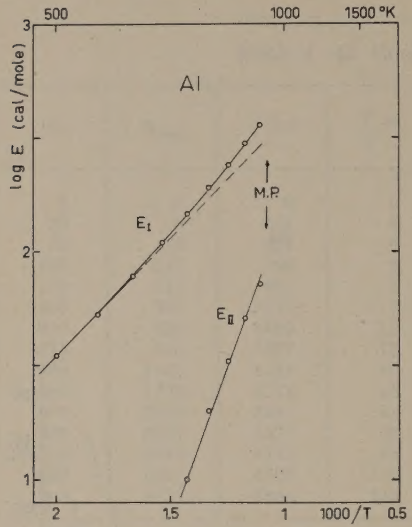

Fig. 9. Separation of the energy of the two kinds of defects in Al.

probably identical. The same agreement exists between the lines for E_I in our figures 3 and 9, and new unpublished results by Åström for Au and Al. The energy observed for Ag in Åström's measurements is for specimen *C* with a grain size of a few mm about 25 % of that calculated from the energy content, and for the specimen *A* with a grain size of 0.3 mm about 6 %. It is imaginable that an ideal crystal would give the whole calculated energy and that in the actual samples only small volume parts are ideal. In the other parts the development of the thermal defects may be catalysed by other imperfections and be too rapid to be observed at least by the used calorimetric method.

9. Remarks concerning the primary defects

The structure of the thermal defects denoted D_I is unknown. The theoretical predictions for vacancies, interstitials or combinations of these elements do not fit the experimental results, from which we point out two characteristic features of the unidentified defects. One is that the heat of formation is rather small, very near to 0.20 eV for the four discussed metals. The other is the fact, found by Åström, that the time constant τ is of the order of hours for the formation of the defects in the undisturbed lattice and that this time constant decreases very little with increasing temperature. The energy of activation as derived from $\log \tau - 1/T$ diagrams is of the order of only 0.05 eV. The extrapolated value of τ for $T \rightarrow \infty$ is still about 10^{16} times the period τ_θ of the atomic vibrations. The formation of a defect at a certain point of the lattice does not therefore imply a very great concentration of the fluctuating thermal energy to this point but a very improbable combination of the movements of a number of atoms. There are several imaginable defects which at first sight seem to comply with this condition. Theoretical evaluations of the heat of formation for different models, which are now going on, will probably help to make the right choice.

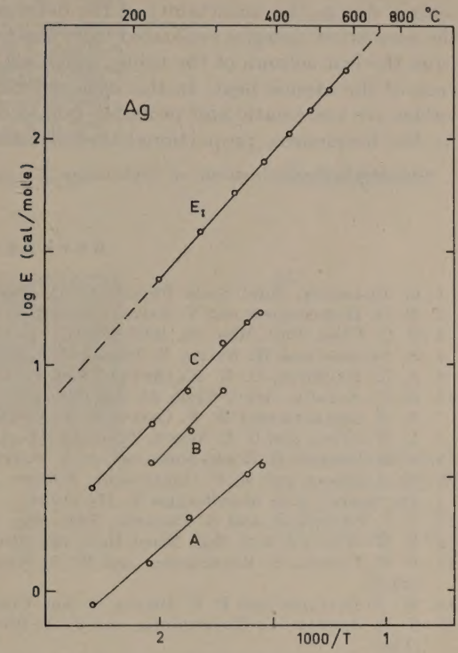

Fig. 10. Comparison of the energy of the unidentified defects in Ag with the calorimetric results obtained by Åström.

10. The zero-point energy

The values of the zero-point energy E_z, obtained from this analysis of the energy content, are probably fairly accurate. In table 5 these values are compared with probably less accurate values obtained earlier in other ways. Two years ago the present writer (20) evaluated the potential half U_z of the zero-point energy from plots of the electrical resistivity as a function of the potential energy due to vibrations and lattice defects. Corresponding zero-point energy-values $2\,U_z$ are inserted in the table together with the differences $2\,U_z - E_z$ in per cent. These differences are probably

Table 5. Zero-point energy in cal/mole.

	E_z	$2\,U_z$	$\frac{9}{8} R\,\theta$	θ
Au	351	340 (−3 %)	425 (+21 %)	190
Ag	403	380 (−6 %)	481 (+19 %)	215
Cu	602	560 (−7 %)	727 (+21 %)	325
Al	730	780 (+7 %)	891 (+22 %)	398

mainly due to the uncertainty of the determinations of $2\,U_z$. The table also contains the zero-point energies evaluated from the Debye theory as $9\,R\theta/8$ using the θ-values from the last column of the table, which are obtained from the temperature dependence of the atomic heat. In this case the differences of about 20 % from the present values are systematic and probably due to deviations from the distribution function for the frequences, proportional to ν^2, contained in the Debye theory.

Stockholm, Royal Institute of Technology.

REFERENCES

1. G. Borelius, Solid State Physics *6*, 65 (1958).
2. H. B. Huntington and F. Seitz, Phys. Rev. *61*, 315 and 325 (1942).
3. F. G. Fumi, Phil. Mag. *46*, 1007 (1955).
4. A. Seeger and H. Bross, Z. Physik *145*, 161 (1956).
5. J. E. Bauerle, C. E. Klabunde, and J. S. Koehler, Phys. Rev. *102*, 1182 (1956).
6. H. U. Åström, Arkiv Fysik *14*, 263 (1958).
7. T. H. Geballe and W. F. Giauque, J. Am. Chem. Soc. *74*, 2368 (1952).
8. D. R. Stull and G. C. Sinke, Thermod. Prop. of Elem., Dow Chem. Co., 1955.
9. F. M. Jaeger, E. Rosenbohm, and J. A. Bottema, Rec. Trav. Chim. Pays Bas *52*, 61 (1933).
10. W. S. Corak and M. P. Garfunkel, 8 Amer. Calorim. Conf. Chicago 1953, Reported by W. De Sorbo, Acta Metallurgica *2*, 274 (1954).
11. F. J. Bradshaw and S. Pearson, Phil. Mag. *2*, 379 (1957).
12. K. K. Kelley, U.S. Bur. Mines Bull. 434 (1941).
13. F. M. Jaeger, E. Rosenbohm, and W. A. Weenstra, Proc. Akad. Wet. Amsterdam *36*, 291 (1933).
14. W. F. Giauque and P. F. Meads, J. Am. Chem. Soc. *63*, 1897 (1941).
15. F. M. Jaeger, E. Rosenbohm, and J. A. Bottema, Proc. Akad. Wet. Amsterdam *35*, 773 (1932).
16. J. A. Kok and W. H. Keeson, Physica *4*, 835 (1937).
17. C. Panseri, F. Gatto, and T. Federighi, Acta Metallurgica *5*, 50 (1957).
18. W. De Sorbo and D. Turnbull, Bull. Am. Phys. Soc. *2*, 262 (1957).
19. F. J. Bradshaw and S. Pearson, Phil. Mag. *2*, 570 (1957).
20. G. Borelius, Arkiv f. Fysik *11*, 291 (1956).

Tryckt den 18 februari 1959

Uppsala 1959. Almqvist & Wiksells Boktryckeri AB